

# **Molecular conduction junctions: Intermolecular effects**

Arie Landau<sup>1</sup>, Leeor Kronik<sup>2</sup> and Abraham Nitzan<sup>1</sup>

<sup>1</sup> School of Chemistry, the Sackler Faculty of Science, Tel Aviv University, Tel Aviv, 69978, Israel

<sup>2</sup> Department of materials and interfaces, Weizmann Institute of Science, Rehovoth, 76100, Israel

## **Abstract**

Intermolecular interactions can affect the conduction properties of molecular junctions in several ways: Direct and through-substrate electronic interactions affect the spectral properties (density of states) of the conducting junction, intermolecular electrostatic interactions affect the positioning of molecular electronic energies and thereby the nature of interface polarization. Such interactions also influence the screening properties of the junction and consequently the electrostatic potential profile across the biased junction. Other consequences include effects on junction mechanical properties that can be manifested by a different temperature dependence of conduction for a single molecule and for a molecular layer, as well as effects on optical response that may be important, for example, for the junction response associated with light induced switching. This article discusses

some of these effects and their implications for the performance of molecular junctions.

## **1. Introduction**

The electronic conduction properties of metal-molecule-metal junctions are determined by the electronic properties of the metal and molecular constituents, the bonding between them, the junction structure and configuration, external electrostatic (gate) fields and environmental parameters such as temperature. The relationship of function and structure offers routes for controlling the junction operation but also results in uncertainties about performance and stability. Characterization of such relationships is therefore central to the study of molecular conduction junctions.<sup>1</sup> One such issue that was already addressed in several experimental and theoretical papers is the dependence of transport on the number of molecules involved in the conduction process. In particular, a comparison between electronic transport of a single molecule junction and that of a junction comprising the corresponding molecular monolayer is of interest. While a common practice is to assume linear scaling with molecular coverage, i.e. to associate the conduction-per-molecule observed in monolayer junctions with that of the single molecule junction, direct experimental and numerical examinations yield mixed observations on this point. On the one hand, clear evidence of linear scaling is indicated by the results of Cui et al<sup>2</sup> and Xu and

Tao<sup>3</sup> in junctions containing 1-5 n-alkane molecules (see Fig. 1).<sup>a</sup> Similarly, Kushmerik and coworkers<sup>4</sup> have found that the current-voltage curves of monolayers of isonitrile oligo(phenylene ethynylene) molecules measured in the cross wire technique with varying contact areas can be scaled to a single curve by dividing with different integers in the range 1-1000, suggesting that the scaled curve corresponds to a single molecule junction. Supporting evidence is obtained by comparing STM and cross wire conduction measurements on a series of saturated and conjugated molecules,<sup>5</sup> where similar current-voltage traces were obtained by using a multiplication factor (of the order of  $10^3$ ) that may account for the different number of molecules in these junctions. On the other hand, the conduction measured in some single molecule junctions was found to be several orders of magnitudes larger than the conduction-per-molecule mentioned in the corresponding monolayers.<sup>6</sup> In a more recent study, Selzer et al<sup>7</sup> have noticed that the small bias conduction per molecule of a molecular layer is similar to that of the corresponding single molecule; however, the differential conductance of the latter increases considerably more rapidly with bias and can become a thousand times larger than the per-molecule layer conductance (see Fig. 2, left panel).

---

<sup>a</sup> In Ref. <sup>3</sup> also 4,4' bipyridine was used with similar results. Note that the conduction values reported by Xu and Tao in these papers are about an order of magnitude larger than those of Cui et al; the difference probably resulting from unrelated technical factors.

Furthermore, the single molecule (1-nitro-2,5-di(phenylethynyl-4'-mercapto)benzene) junction shows temperature dependence with transition to activated conduction at  $T > 100\text{K}$ , while the conduction of the corresponding molecular layer remains temperature independent up to room temperature (Fig. 2, right panel). Obviously, the effect of intermolecular interactions depends on the nature of the adsorbed molecules. A recent scanning tunneling spectroscopy study<sup>8</sup> of monolayers of 3,4,9,10-perylenetetracarboxylicacid- dianhydride (PTCDA) on a silver substrate showed a remarkable electronic band dispersion (see Fig. 3) associated with the layer electronic structure, indicating a free electron behavior with an effective mass of  $m_{eff} = 0.47m_e$  ( $m_e$  is the free electron mass). This surface electron delocalization indicates strong intermolecular coupling that has been attributed by the authors to mostly through-metal interaction. The existence of such strong intermolecular coupling suggests that conduction in this system will not scale linearly with that of single-molecule junctions based on the same molecule.

---

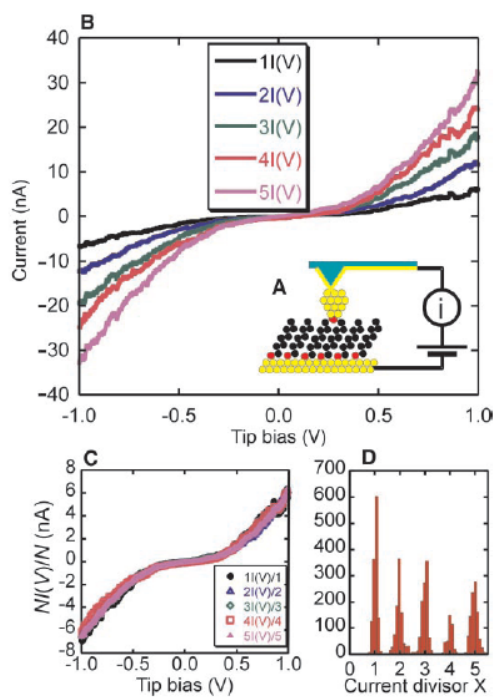


Fig. 1. Conduction of 1,8-octanedithiol molecule in the configuration shown in A. (after Cui et al<sup>2</sup>). Several conductance characteristics (B) collapse into a single line following scaling by intergers from 1 to 5 (C). D shows an histogram of conductance signals.

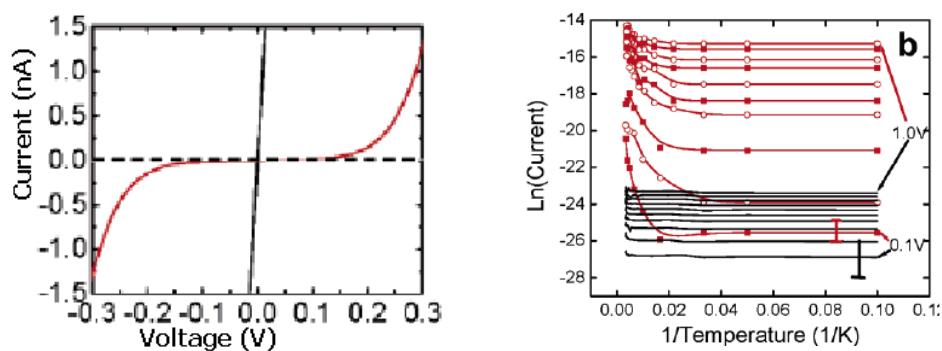


Fig. 2. Conductance of 1-nitro-2,5-di(phenylethynyl)-4'-mercapto benzene between gold leads. Left: Red – single molecule; black – molecular layer. Dashed black is the molecular layer signal normalized per molecule. Right: Temperature and voltage dependence of conduction. Red – single molecule; black – molecular layer per molecule. From Selzer et al<sup>7</sup>.

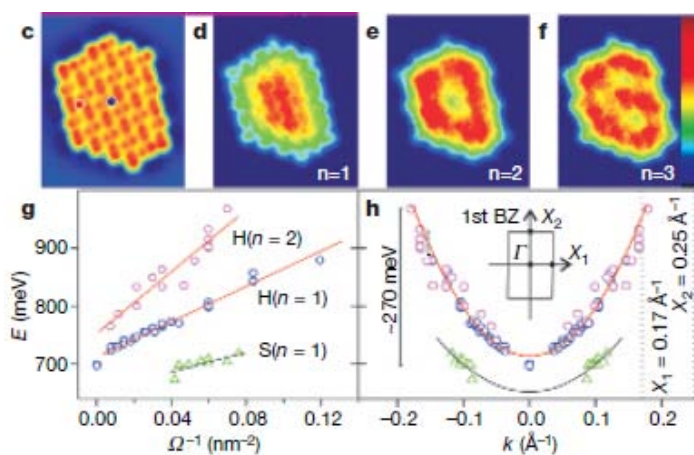


Fig. 3. Top panels: Scanning tunneling images of monolayers of 3,4,9,10 perylenetetracarboxylic acid-dianhydride on a silver substrate, showing different electronic states in the confined island geometry. Bottom Panels: The size dependent energy (left) can be translated into an electronic band dispersion (right) associated with the layer electronic

structure, indicating a free electron behavior with an effective mass of  $m_{eff} = 0.47m_e$ . From Temirov et al<sup>8</sup>.

Theoretical studies of this issue also lead to varied results. Early studies by Magoga and Joachim<sup>9</sup> concluded that linear scaling of the conduction  $g(N)$  with the number  $N$  of identical molecules connecting the leads exists in the form

$$g(N) = Ng_{eff}(1), \quad (1)$$

where the effective single molecule conduction  $g_{eff}(1)$  differs from the corresponding single molecule property  $g(1)$  because of intermolecular interactions. The latter can be direct interactions between neighboring molecules or interactions resulting from their mutual coupling to the leads. Obviously, however,  $N$  has to be large enough for Eq. (1) to hold. In the non-resonant small bias regime  $g_{eff}(1) > g(1)$ , because intermolecular interaction brings molecular states density closer to the Fermi energy of the lead. Yaliraki and Ratner<sup>10</sup> have made a similar observation by comparing the conduction of two parallel molecular wires to that of a single wire. On the other hand, Lang and Avouris<sup>11</sup> have studied the low bias conduction of a junction containing two carbon wires connecting jellium leads as a function of the interwire separation. A non-monotonic distance dependence, with an overall conduction increase at larger separation was found and rationalized

in terms of the effect of the interwire interaction on the molecular density of states at the Fermi energy. The magnitude of the effect should depend on the adsorbate molecules. Indeed, Kim<sup>12</sup> et al have studied the conduction of junctions based on single molecules and molecular layers of Hexane-dithiolate between Au(111) electrodes and found that the effect of intermolecular coupling on conduction is negligible in these junctions.

Effects of intermolecular interactions on properties of molecular junctions can arise from several sources. Clearly, direct interactions between the molecules may affect the transport properties of a molecular layer, as can indirect interactions mediated by the underlying substrate. Such interactions may directly affect transport, but may also influence transport properties by affecting the molecular configuration and its response to the imposed bias potential and to temperature change. Electrostatic effects are particularly noteworthy, having at least two important effects. First, the way an imposed bias is distributed across the junction depends on the lateral dimension of the bridging layer in a way that reflects the layer screening properties.<sup>13,14</sup> In turn, the way by which the bias potential falls along the junction has important implications on the junction transport properties, see, e.g. Refs. <sup>15</sup> and <sup>16</sup>. Secondly, polar adsorbate molecules, or molecules that form polarized adsorption sites because of charge transfer to/from the substrate are expected

to show strong intermolecular interaction effects,<sup>17-20</sup> as discussed in Section 3.

Finally, intermolecular interactions affect the manifestations of other transport properties that bear on the performance of molecular conduction junctions. For example, junction stability is related to its structural response to the imposed field and ensuing current, as well as to its temperature rise during conduction. The latter depends on the junction ability to dissipate excess energy, which in turn depends on its immediate environment. In particular, large differences may exist between a junction that can dissipate heat only through the contacting electrodes (as with a single molecule connecting metal leads in vacuum) or also through lateral interactions with neighboring molecules (a situation associated with molecular layers and junctions embedded in solvent environments). As another example, optical control, a desired property in molecular devices, relies on the system optical response which is expected to be a sensitive function of the nature and structure of its molecular interface.

This paper focuses on several of the above mentioned aspects of single molecule versus molecular island and layer behavior of molecular junctions. In section 2, we briefly outline a simple generic model for the effect of molecular island size on the potential distribution along a biased junction. In Section 3, we review theoretical calculations of charge transfer at the interface of

semiconductors and polar molecules. In Section 4, we present a generic study of effects associated with short range intermolecular and molecule-substrate interactions on the transport properties of single molecules and the corresponding molecular islands and layers. We use a minimal model of single-level molecules connecting electrodes characterized by simple cubic lattices in order to examine the effect of intermolecular interactions on the junction spectral function and conduction properties. Section 5 concludes.

## **2. Electrostatics: the bias potential distribution along the junction**

Understanding the potential bias distribution along a molecular junction is necessary for understanding and predicting its conduction behavior. A demonstration of the importance of this issue to the understanding of the current-voltage behavior of molecular junctions was first presented by Datta and coworkers.<sup>15,21</sup> They have shown, within a simple Extended-Hückel (EH) model for  $\alpha,\alpha'$ -xylyl dithiol bridging between two gold leads, that the potential profile (imposed on the molecule as input to the EH calculation) had a profound effect on quantitative as well as qualitative aspects of the calculated current-voltage

characteristic. Since then, the evaluation of the electrostatic potential along the junction has become an integral part of a full scale self consistent calculation.<sup>22</sup> On the experimental side, Bachtold et al<sup>23</sup> have used scanned probe microscopy of both single-walled and multi-walled carbon nanotubes (SWNTs and MWNTs) to measure the potential drop along such nanotubes connecting between two gold electrodes. They found an approximately linear drop of the potential in a MWNT of diameter 9nm while for a metallic SWNT bundle of diameter 2.5nm the potential was flat beyond the screening regions at the tube edges. A theoretical analysis of this behavior was provided in Ref. <sup>24</sup>. While these experiments cannot be related directly to the calculations discussed above (the nanotube length is a few microns and impurity and defect scattering may be effective as is most certainly the case in the MWNT measurement), the flat potential seen in the metallic SWNT measurement is in fact a remarkable observation implying a very long mean free path ( $>1\mu\text{m}$ ) for electrons in these room temperature structures.

As indicated by the above discussion, the computational methodology for evaluating the potential distribution on a specified biased molecular wire is available. Here we focus on a generic issue pertaining to our theme: the dependence of this distribution on the wire lateral cross-section. For a single molecule junction the cross-section radius is of order of 1-2Å and its increases

linearly with the number of molecules connecting between the leads. To see the effect of this lateral wire width on the screening that affects the potential distribution, Nitzan et al<sup>13</sup> have employed a maximum screening model: The molecular wire is modeled as a cylinder characterized by the molecular length  $L$  and cross-section diameter (molecular wire thickness)  $\sigma$ , perpendicular to and connecting between two planar metal electrode surfaces. The cylinder is oriented parallel to the  $z$  axis, with its axis going through the origin in the  $xy$  plane. For simplicity, the electrodes are taken to be blocking, so there is no current through the junction, and the potentials at the wire-electrode interface are set to be  $\Phi_1$  and  $\Phi_2$  at  $z=-L/2$  and  $z=L/2$ , respectively. It is further assumed that screening is described by a Thomas-Fermi model

$$\nabla^2\Phi = -4\pi\rho(\mathbf{r}) = -\lambda^{-2}\Phi \quad (2)$$

with the molecular screening length  $\lambda$  taken to be a model parameter. Finally, taking the direction perpendicular to the metal electrode planes to be  $z$ , and  $\mathbf{r}_{\parallel}$  to denote the lateral direction, a solution is sought in the form

$$\Phi(\mathbf{r}_{\parallel}, z) = F(\mathbf{r}_{\parallel})\Phi(0, 0, z)$$

where the function  $F(\mathbf{r}_{\parallel})$  is chosen to describe the lateral confinement of the charge distribution in the molecular cylinder. This leads to

$$\Phi(0,0,z) = \Phi_0(z) - \frac{\Delta\Phi}{\pi} \times \sum_{\substack{n=0 \\ (\text{even})}}^{\infty} \frac{(-1)^{n/2}}{n} \frac{F_n}{1+F_n} \sin\left(\frac{2\pi n}{L}z\right) \quad (3)$$

where (with  $\Phi_1$  and  $\Phi_2$  the potentials at the two boundaries)

$$\Phi_0(z) = \frac{1}{2}(\Phi_2 + \Phi_1) + \frac{z}{L}\Delta\Phi \quad ; \quad \Delta\Phi = (\Phi_2 - \Phi_1) \quad (4)$$

and

$$F_n = \frac{1}{\lambda^2} \int \frac{d^2\mathbf{k}}{(2\pi)^2} \frac{\hat{F}(\mathbf{k}_{\parallel})}{k_{\parallel}^2 + (2\pi n/L)^2} \quad ;$$

$$\hat{F}(\mathbf{k}_{\parallel}) = \int d^2\mathbf{r}_{\parallel} e^{-i\mathbf{k}_{\parallel}\cdot\mathbf{r}_{\parallel}} F(\mathbf{r}_{\parallel}) \quad (5)$$

Using for the confinement function the model form

$$F(\mathbf{r}_{\parallel}) = e^{-(r_{\parallel}/2\sigma)^2} \quad (6)$$

(note that this function is not normalized and describes a charge density at the cylinder axis independent of the width  $\sigma$ , as desired when the cylinder models a molecular assembly of a given diameter) leads to the results shown in Figure 4,<sup>13</sup> where  $\Phi_1 = -\Delta\Phi/2$ ,  $\Phi_2 = \Delta\Phi/2$  are used.

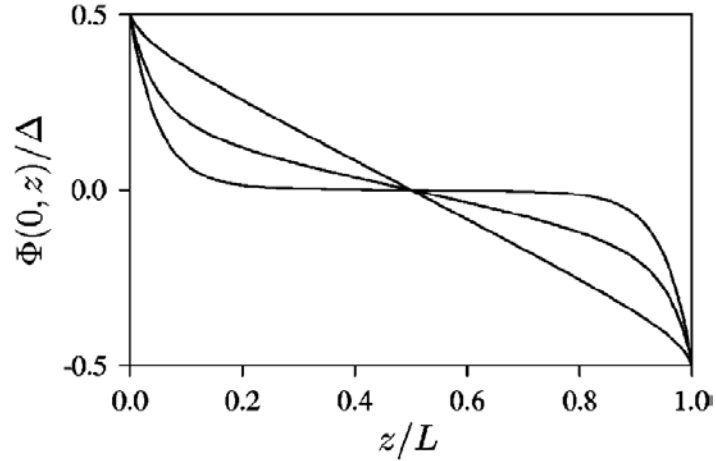


Figure 4. The potential profile along a molecular wire computed from Eqs. (3) - (6) is shown for a screening length  $\lambda/L = 0.05$ . The thickness parameter  $\sigma/L$  takes the values 0.0125, 0.05, and 0.5 from the almost linear behavior to the voltage profile containing almost a plateau. From Nitzan et al.<sup>13</sup>

These results show that the wire thickness, determined by the number of molecules connecting in parallel between the conducting leads, does constitute an important generic attribute that determines the general behavior of the potential bias distribution along a molecular wire. Obviously, a Thomas-Fermi screening model is not a good representation of electrostatic screening in molecular systems. However, it suffices for demonstrating this point. Indeed, detailed molecular level calculations<sup>14</sup> of the potential profile in molecular junctions show similar behavior.

### **3. Molecule - substrate charge transfer**

At thermodynamic equilibrium, uniformity in the electronic chemical potential in a system comprising a conducting substrate and an adsorbed molecule, molecular island or a molecular layer is achieved by (partial) electronic charge transfer between the molecular adsorbate and the underlying substrate. This charge transfer results in a contribution to the surface dipole density, which is manifested as a change in the substrate work function but should also affect the potential profile in a biased molecular junction. Obviously, the energetic balance that determines the magnitude and direction of the transferred charge depends strongly on the electrostatics within the created dipole layer. For this reason we may expect a strong dependence of this process on the number and density of the molecules involved.

A demonstration of this expectation was recently made in calculations of molecules and molecular monolayers adsorbed on silicon.<sup>18,19</sup> Two types of systems were considered. In one a molecular monolayer (calculations with several benzene derivatives were done) is adsorbed on Si (111) surface.<sup>18</sup> The substrate is represented by a slab with thickness of at least six Si atomic layers embedded in a 3-dimensional periodic supercell. Density functional theory is used in the local density approximation where the Kohn-Sham equations are solved using a plane wave basis set.

The other system type considered is a Si cluster (with several tens of Si atoms) with one adsorbed molecule. When such a cluster is large enough this is a model for a single molecule adsorbed on Si surface. The dipole per adsorbed molecule was computed and compared.

Results of these calculations are shown in Figures 5 (slab/monolayer system) and 6 (cluster with single adsorbate molecule), which depict, for several benzene derivatives, the dipole moment per adsorbed molecule against the dipole moment of the isolated (gas phase) molecule. The most important difference between the results displayed in these figures is the fact that the slope of the lines in Fig. 5 are smaller than one, indicating that the dipole per molecule in an adsorbate layer is smaller than the corresponding isolated molecule case, while the slopes in Fig. 6 are larger than 1. This indicates different charge reorganization mechanisms that result in a larger surface dipole in the case of a single adsorbed molecule and a smaller one in the molecular layer. The slab/molecular-layer observation can be rationalized in terms of the tendency to increase system stability by reducing dipole-dipole repulsion in the molecular layer case,<sup>20</sup> and is consistent with the dependence of the slopes in fig. 5 on the surface coverage. Calculations show that charge migration between the molecules and the substrate is very small in this case (which is consistent with the electric field suppression outside the layer<sup>20</sup>) and dipole

reduction is achieved by depolarization of the molecules themselves. In the cluster/single molecule case the surface dipole enhancement is caused mainly by (cluster size dependent) electron exchange with the Si substrate in the direction that depends on the electron withdrawing/donating property of the molecule. This implies that the net polarization should be a strong function of coverage – a prediction confirmed in recent experimental work.<sup>25</sup> It is interesting to note<sup>20</sup> that electron transfer in the opposite direction is expected in the complementary case, where molecules are *absent* from a molecular monolayer, a phenomenon that often occurs naturally.<sup>26</sup> Indeed, the superposition principle tells us that the electric field near a pinhole of an otherwise perfect dipolar monolayer is simply the difference between the electric field of the perfect monolayer and the electric field of the “missing domain”. Therefore the electrostatic field of a single-molecule hole in such a monolayer, beyond the field suppression distance (of order of the intermolecular distance in the layer), is very similar to that of a single dipole in the *opposite* direction, implying similar reversal in the direction of charge transfer.

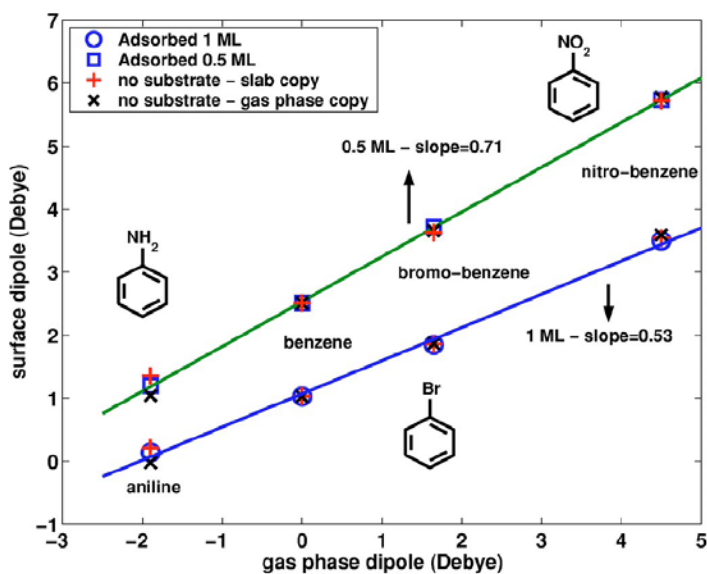


FIG. 5. Surface dipole per molecule as a function of gas-phase molecular dipole for a self assembled monolayer (SAM) of benzene derivatives with various functional groups,<sup>18</sup> for both 1 ML and 0.5 ML coverage. For each coverage, dipoles were computed for a SAM/substrate configuration, for a SAM with the substrate removed, but with molecules in their relaxed surface-adsorbed geometry, and for a SAM with the substrate removed and the molecules in their relaxed gas-phase geometry. For ease of comparison all curves were shifted such that the dipole moment of the benzene SAM is the same.

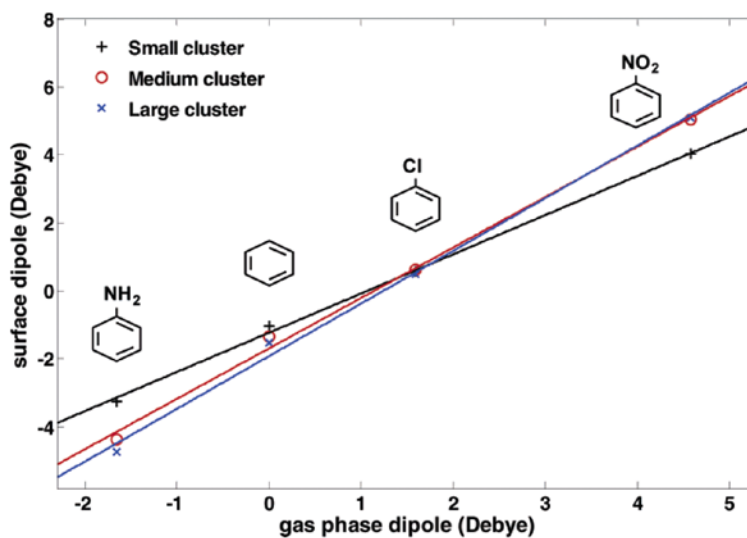


Fig. 6. Same as Fig. 5 for a single molecule adsorbed on silicon clusters of different sizes.<sup>19</sup> Using linear regression, slopes of 1.15, 1.48, and 1.55 are found for the “small” (1 atom), “medium” (14 Si atoms), and “large” (38 Si atoms) clusters, respectively.

#### 4. Spectral and conduction properties of molecules and molecular layers

When a junction comprises several molecules connecting in parallel between the two leads, intermolecular effects arise from direct as well as from substrate mediated interactions. Here we examine the consequences of such interactions on the spectral and conduction properties of the molecular junction, using a simple tight binding model for the leads as well as for the molecular conductor. The following discussion focuses on metal-molecule-

metal junctions. An equivalent analysis of junctions involving semiconductor electrodes was recently published.<sup>27</sup> Our aim is to compare the spectral properties (molecule projected density of states (DOS)) of, and the conduction associated with, a molecular monolayer (ML, Fig. 7), a finite molecular island (IL) and a single molecule (SM) chemisorbed on a metal surface. The metal is described by a tight binding model defined on a simple-cubic cell structure characterized by a lattice constant,  $a$ , which is semi-infinite in the  $Z$  direction perpendicular to the metal surface. Periodic boundary conditions are used in the  $X$  and  $Y$  directions (see Fig. 7). Both metal and molecular system are described by simple nearest-neighbor (nn) tight-binding models. Each metallic atom is represented by a single orbital  $|n_x, n_y, n_z\rangle$ , coupled to its nearest neighbor orbitals. A similar description is also used for the molecular system and for the molecule–metal interaction. The model is characterized by the molecular and metal site energies,  $\varepsilon_m$  and  $\varepsilon_t$ , respectively, and by the interaction between neighboring metal sites,  $V^{(t)}$ , neighboring molecules,  $V^{(m)}$ , and nearest-neighbor metal-molecule interaction  $V^{(mt)}$ . The model Hamiltonian  $\hat{H} = \hat{H}^{(m)} + \hat{H}^{(t)} + \hat{H}^{(mt)}$  has the usual nn tight binding form where, e.g., the molecule-metal interaction is given by

$$\hat{H}^{(mt)} = V^{(mt)} \sum_{n_x} \sum_{n_y} \left[ \left| n_x n_y (n_z = 0) \right\rangle \left\langle n_x n_y (n_z = 1) \right| + h.c. \right]. \quad (7)$$

The sum over the lateral indices  $n_x, n_y$  is over the occupied sites of the molecular adsorbate,  $Z=0$ , plane. More than one coupling parameter  $V^{(mt)}$  may be needed to describe more complex layer structures.

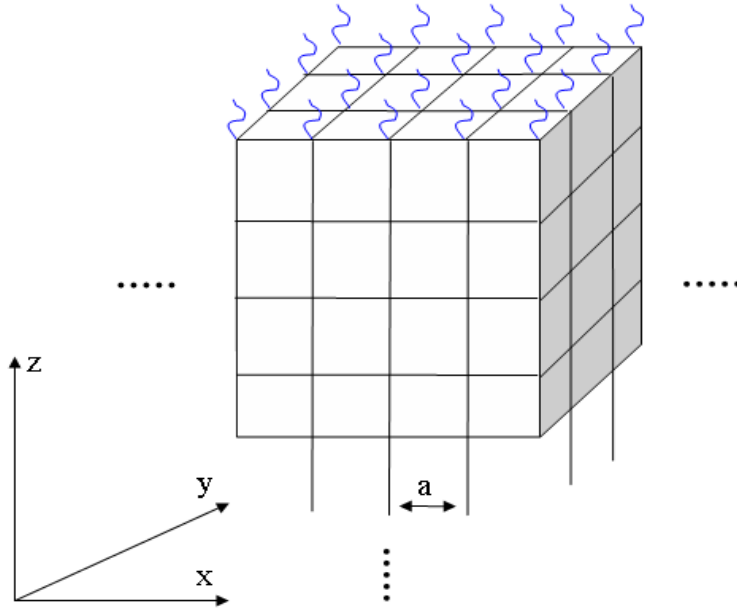


Fig. 7. Schematic cartoon of a simple 1:1 ML (curly lines represent molecules) adsorbed on a metallic electrode (grid points represent metallic-atoms). The Z direction is normal to the surface, X and Y are parallel to it,  $a$  is the unit distance. The cubic lattice is  $(n_x = -\infty \dots \infty, n_y = -\infty \dots \infty, n_z = 0 \dots \infty)$  and the molecular layer occupies the sites  $(n_x, n_y, 0)$ .

It is convenient to replace the local basis  $|n_x, n_y, n_z\rangle$  by a basis in which Bloch wavefunctions are used in the X, Y directions:

$$|\theta_x \theta_y n_z\rangle = \frac{1}{\sqrt{N_x N_y}} \sum_{n_x=-(N_x/2)}^{(N_x/2)-1} \sum_{n_y=-(N_y/2)}^{(N_y/2)-1} e^{i(\theta_x n_x + \theta_y n_y)} |n_x n_y n_z\rangle, \quad (8)$$

where  $\theta_u = k_u a$ , and  $k_u = 2\pi j / N_u$  ( $j=1, 2, \dots, N_u$ ;  $u=x, y$ ).

In what follows we also use the notation  $\boldsymbol{\theta}_{xy} = (\theta_x, \theta_y)$ . For a pure metal this transformation diagonalizes the Hamiltonian, yielding the energy eigenvalues

$$E_t(\boldsymbol{\theta}_{xy}) = \varepsilon_t + 2V^{(t)} (\cos \theta_x + \cos \theta_y) \quad (9)$$

The spectral and transport properties we seek can be obtained from the surface Green function (GF),  $G^{(ts)}$ , and the associated surface self energy (SE),  $\Sigma^{(ts)}$ . Details of the calculation are given in Ref. <sup>28</sup> and only an outline is given below. For the bare metal surface these are given by

$$G_{\boldsymbol{\theta}_{xy}}^{(ts)}(E) = \left( E - E_t(\boldsymbol{\theta}_{xy}) - \Sigma_{\boldsymbol{\theta}_{xy}}^{(ts)}(E) \right)^{-1} \quad (10)$$

and

$$\Sigma_{\mathbf{\theta}_{xy}}^{(ts)} = V^{(t)} G_{\mathbf{\theta}_{xy}}^{(ts)} V^{(t)} \quad (11)$$

Eqs. (10) and (11) can be solved for the metal surface GF iteratively. In addition, the surface spectral density function of the metal is defined as

$$\Gamma_{\mathbf{\theta}_{xy}}^{(ts)}(E) = -2 \operatorname{Im} \left[ \Sigma_{\mathbf{\theta}_{xy}}^{(ts)}(E) \right] \quad (12)$$

Similarly, for a simple<sup>b</sup> adsorbed monolayer (top layer in Fig. 7) the GF,

$$G_{\mathbf{\theta}_{xy}}^{(ml)}(E) = \left( E - E_m(\mathbf{\theta}_{xy}) - \Sigma_{\mathbf{\theta}_{xy}}^{(ml)}(E) \right)^{-1} \quad (13)$$

where

$$E_m(\mathbf{\theta}_{xy}) = \varepsilon_m + 2V^{(m)}(\cos \theta_x + \cos \theta_y) \quad (14)$$

and

$$\Sigma_{\mathbf{\theta}_{xy}}^{(ml)} = V^{(mt)} G_{\mathbf{\theta}_{xy}}^{(ts)} V^{(mt)} \quad ; \quad \Gamma_{\mathbf{\theta}_{xy}}^{(ml)}(E) = -2 \operatorname{Im} \left[ \Sigma_{\mathbf{\theta}_{xy}}^{(ml)}(E) \right] \quad (15)$$

When the molecular layer is in contact with two metals, L and R, with the same simple 1:1 adsorption geometry, the ML SEs combine additively,  $\Sigma_{\mathbf{\theta}_{xy}}^{(ml)} = \Sigma_{\mathbf{\theta}_{xy}}^{(ml,L)} + \Sigma_{\mathbf{\theta}_{xy}}^{(ml,R)}$ , where

$$\Sigma_{\mathbf{\theta}_{xy}}^{(ml,K)} = V^{(mt,K)} G_{\mathbf{\theta}_{xy}}^{(ts,K)} V^{(mt,K)} \quad ; \quad K = L, R. \quad (16)$$

In the following we also require the position space (XY) representation of these functions. In particular the local site GF

$$G_{\mathbf{n}_{xy}, \mathbf{n}_{xy}}^{(ml)}(E) = \frac{1}{4\pi^2} \int_0^{2\pi} \int_0^{2\pi} d\theta_x d\theta_y G_{xy}^{(ml)}(E), \quad (17)$$

is related to the local density of states (DOS) per molecule

$$\rho^{(ml)}(E) = -\frac{1}{\pi} \text{Im} \left[ G_{\mathbf{n}_{xy}, \mathbf{n}_{xy}}^{(ml)}(E) \right]. \quad (18)$$

Equivalent expressions can be obtained when instead of a homogeneous molecular layer we have a molecular island of  $J$  molecules ( $J=1$  corresponds to a single adsorbed molecule) adsorbed on the metal surface and interacting with  $N$  surface atoms. Denote the corresponding interaction elements by  $V_{nj}^{(mt)}$ ;  $n = 1, \dots, N$ ;  $j = 1, \dots, J$ . Note that there is a one-to-one correspondence between  $n$  and a position  $\mathbf{n}_{xy}$  on the metal surface. However, we have dropped the requirement of “simplicity” as defined above<sup>b</sup> with respect to the adsorbate island or ML. The molecular island Hamiltonian,  $\hat{H}^{(il)}$ , is a combination of a diagonal part,  $\varepsilon_m \mathbf{1}_J$ , where  $\mathbf{1}_J$  is a unit matrix of order  $J$ , and a non-diagonal part associated with the interactions  $V^{(m)}$  between island molecules. The island GF (a  $J \times J$  matrix in the position representation) is now given by

$$G^{(il)}(E) = \left( E - \hat{H}^{(il)} - \hat{\Sigma}^{(il)} \right)^{-1} \quad (19)$$

where the island SE is given by

---

<sup>b</sup> By “simple” we mean that each adsorbed molecule is coupled to only one metal surface

$$\Sigma_{j,j'}^{(il)} = \sum_n^N \sum_{n'}^N V_{jn}^{(mt)} G_{n,n}^{(ts)} V_{n'j'}^{(mt)} ;$$

$$\Gamma_{j,j'}^{(il)}(E) = i \left( \Sigma_{j,j'}^{(il)} - \Sigma_{j,j'}^{(il)\dagger} \right) \quad (20)$$

and may be easily evaluated for any finite island once the metal surface GF (Eq. (10)) has been calculated. Again, when the molecular island connects between two metals the self-energy in (19) is the sum  $\Sigma^{(il,L)} + \Sigma^{(il,R)}$ , where

$$\Sigma_{j,j'}^{(il,K)} = \sum_n^N \sum_{n'}^N V_{jn}^{(mt,K)} G_{n,n'}^{(ts,K)} V_{n'j'}^{(mt,K)} ; \quad K = L, R. \quad (21)$$

With these results we can compare spectral properties of infinite and finite molecular layers, down to a single molecule. For example, a relationship between the per molecule DOS associated with a single adsorbed molecule,  $\rho^{(sm)}(E)$ , and the corresponding function of a molecular layer  $\rho^{(ml)}(E)$  is obtained in the form<sup>28</sup>

$$\frac{\rho^{(sm)}(E)}{\rho^{(ml)}(E)} = \frac{\text{Im} \left[ \left( E - \varepsilon_m - \frac{1}{4\pi^2} \int_0^{2\pi} \int_0^{2\pi} d\theta_x d\theta_y \Sigma_{\mathbf{\theta}_{xy}}^{(ml)}(E) \right)^{-1} \right]}{\text{Im} \left[ \frac{1}{4\pi^2} \int_0^{2\pi} \int_0^{2\pi} d\theta_x d\theta_y \left( E - E_m(\mathbf{\theta}_{xy}) - \Sigma_{\mathbf{\theta}_{xy}}^{(ml)}(E) \right)^{-1} \right]} \quad (22)$$

---

atom, and vice versa.

Next, consider conduction properties of these molecular systems when placed between two metal electrodes. According to the Landauer formula,<sup>29</sup> conduction in the linear response limit is given by  $(e^2 / \pi \hbar) \mathbb{T}(E_F)$  where the transmission coefficient  $\mathbb{T}(E)$  is given in terms of the GF and the SE of the subsystem comprising the molecular bridge

$$\mathbb{T}(E) = \text{Tr}_{\text{bridge}} \left[ \Gamma^{(L)}(E) G(E) \Gamma^{(R)}(E) (G(E))^\dagger \right] \quad (23)$$

$\text{Tr}_{\text{bridge}}$  stands for a trace over the states of the bridging system. For a finite molecular island this trace is easily evaluated in the representation of local island states  $j$ , using Eqs. (19) and (20). In particular, for a single molecule junction this yields

$$\mathbb{T}^{(sm)}(E) = \Gamma^{(sm,L)}(E) G^{(sm)}(E) \Gamma^{(sm,R)}(E) (G^{(sm)}(E))^\dagger \quad (24)$$

For the simple molecular layer the transmission *per molecule* (denoted  $\mathbb{T}^{(ml)}(E)$  below) is given by

$\left\langle \mathbf{n}_{xy} \left| \Gamma^{(L)}(E) G(E) \Gamma^{(R)}(E) (G(E))^\dagger \right| \mathbf{n}_{xy} \right\rangle$ , where  $\mathbf{n}_{xy}$  corresponds

the lateral position of any one molecule on the ML. This leads to

$$\mathbb{T}^{(ml)}(E) = \frac{1}{4\pi^2} \int_0^{2\pi} \int_0^{2\pi} d\theta_x d\theta_y \Gamma_{\mathbf{\theta}_{xy}}^{(ml,L)}(E) G_{\mathbf{\theta}_{xy}}^{(ml)}(E) \Gamma_{\mathbf{\theta}_{xy}}^{(ml,R)}(E) (G_{\mathbf{\theta}_{xy}}^{(ml)}(E))^\dagger \quad (25)$$

Once the transmission function (24) or (25) has been obtained, we can also compute the current through the junction using the Landauer formula,

$$I(\Phi) = \int dE (f_L(E) - f_R(E)) \mathbb{T}^{(M)}(E, \Phi) \quad (26)$$

Where  $M$  stands for a single molecule (SM), a molecular island (IL) or a molecular monolayer (ML), and where  $f_L(E)$  and  $f_R(E)$  are the Fermi functions of the left and right electrode, respectively.

$$f_K(E) = \left( 1 + \exp\left(\frac{E - \mu + e\Phi^K}{k_B T}\right) \right)^{-1}; \quad K = L, R, \quad (27)$$

where  $\mu$  is the unbiased Fermi energy,  $\Phi^K$  is the potential on the electrodes  $K = L, R$ , and  $k_B$  and  $T$  are the Boltzmann constant and the temperature, respectively. In the calculation reported below we set  $\Phi^L = 0$  and denote  $\Phi^R = \Phi$ . The latter assignment is expressed by shifting all metal sites energies on the right by  $-e\Phi$ . The molecular site energy is then taken as  $\varepsilon_m(\Phi) = \varepsilon_m(0) - S e \Phi$  where the shift parameter  $0 \leq S \leq 1$  reflects a particular assumption about the way by which the bias voltage falls along the molecular bridge.

Figures 8-10 show some results based on this model, using model parameters that reflect orders of magnitude of physical observables such as metallic band widths, computed interaction

energies between adsorbate molecules, and lifetimes of excess electrons on molecules adsorbed on metal surfaces (see Ref. <sup>28</sup>).

Figure 8 depicts results obtained for the transmission coefficient (Eq. (23)) per molecule, through a molecular monolayer with (white circles) and without (black circles) direct intermolecular interactions. Also shown is the transmission coefficient through a single adsorbed molecule. The difference between the two latter results stems from the fact that molecules interact with each other, even in the absence of direct interactions, through their mutual interactions with the underlying metal.

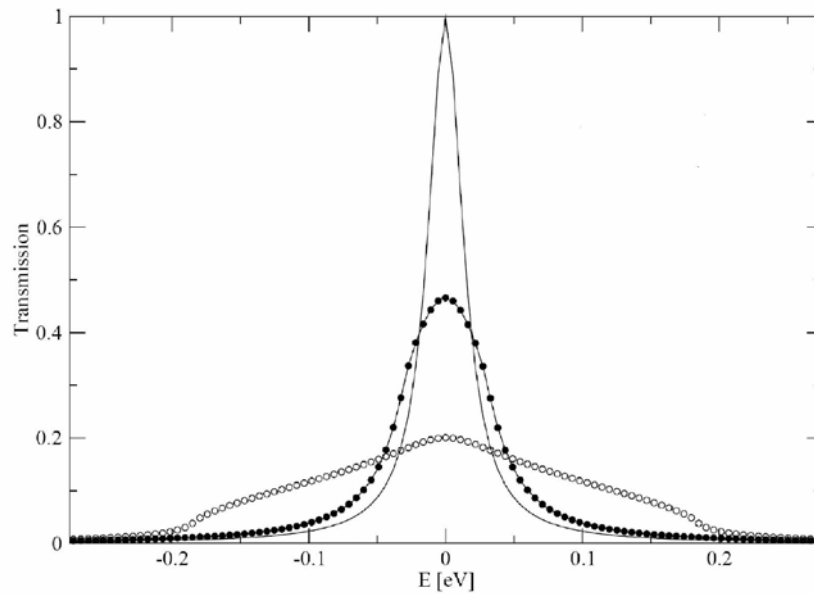


Fig. 8 White circles: Transmission (per molecule) as function of energy through a ML, calculated with model parameters  $V^{(i)} = 0.03 \text{ a.u.} \sim 0.82 \text{ eV}$ ,  $V^{(m)} = 0.0035 \text{ a.u.} \sim 0.095 \text{ eV}$ ,  $V^{(mt)} = 0.004 \text{ a.u.} \sim 0.11 \text{ eV}$  and

$\varepsilon_m = \varepsilon_t = 0$ . Black circles: Same, except with  $V^{(m)} = 0$ . Full line: The transmission coefficient through a single molecule using the same parameters ( $V^{(m)}$  is irrelevant in this case).

The most significant effect of intermolecular interactions on the transmission coefficient is the considerable broadening of the transmission resonance associated with the molecular level. With our choice of parameter the direct intermolecular interaction plays a dominant role in this broadening, even though through metal interaction has a non-negligible effect, as suggested in Ref. <sup>8</sup>.

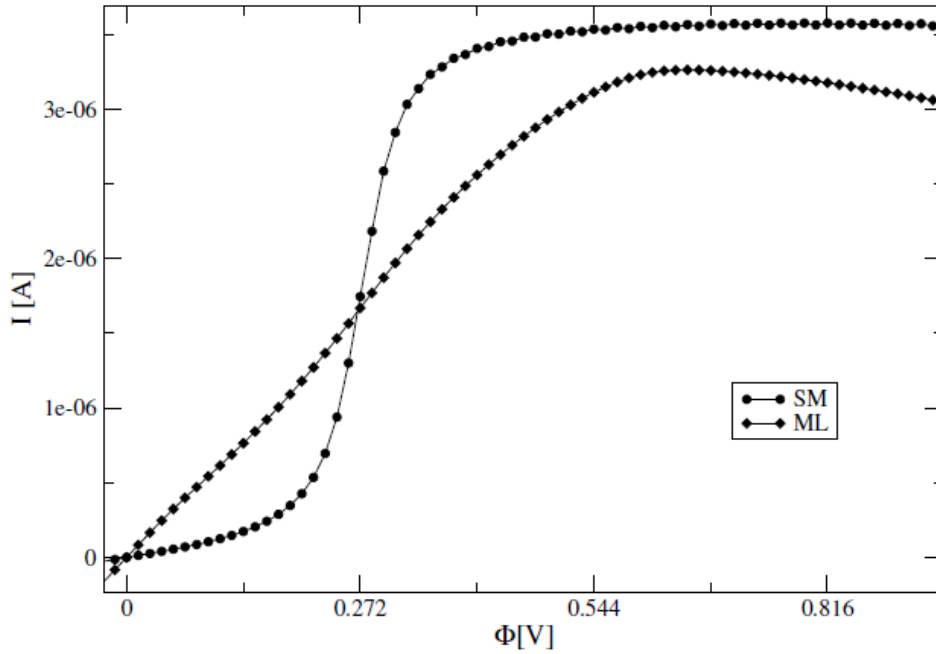


Fig 9. Current  $I$  (per molecule) as function of the bias voltage  $\Phi$  via a SM (circles) and ML (diamonds), with the molecular level set at  $\varepsilon_m = -0.136\text{eV}$ .  $\varepsilon_t$ , taken as the energy origin is also the Fermi energy in this

calculation (corresponding to a monovalent metal). In this system  $I(\Phi) = I(-\Phi)$  and only the  $\Phi > 0$  side is shown.

Fig. 9 shows the consequence of this broadening on the current-voltage characteristics of the junction, computed using (26) with the molecular-shift parameter  $S=0.5$ . When the molecular site-energy is well within the Fermi window, the SM current is higher than the current per molecule through a ML, because part of the broadened layer spectral density is outside that window. In the opposite case the molecular resonance may lie outside the Fermi window while the layer band may be broad enough to ‘spill’ into the window. The layer conductance will be higher in this case. Thus, in the case where  $\varepsilon_m = -0.136$  eV and  $S = 0.5$  the molecular level enters the Fermi window at  $\Phi = 0.272$  V, and for lower bias the ML current is higher than its SM counterpart. This is reversed above  $\Phi = 0.272$  V, where the SM spectrum is better contained within the Fermi window. The decrease in the ML current at higher voltages is a manifestation of the fact that the broadened layer spectrum starts to ‘feel’ the metallic band edge so that the tail of the molecular band that extends beyond this edge cannot contribute to conduction. Again, level broadening arguments make it clear that such an effect will occur in a molecular layer at lower voltages than in the SM case.

Next, consider the scaling of conduction with the number of conducting molecules. Experimentally, such considerations pertain to two possible situations: (A) an essentially infinite molecular layer is engaged by a probe (or probes) that connect to a varying number of molecules, and (B) the junction involves molecular islands of varying sizes. In both cases we find that linear scaling appears only beyond some characteristic island size that depends on the strength of intermolecular interactions. Figure 10 demonstrates this behavior in case B. To ease the computational effort a two-dimensional junction model is considered in which the surface and the adsorbed molecular layers are represented by 1-dimensional rows of sites. The molecules are taken to couple more strongly to one of the electrodes (“substrate”) than to the other (probe). Also, the tight binding parameter for the 2-dimensional “metal” is taken to be large enough to yield a sufficiently large metal bandwidth. Our results show strong dependence on the molecular island size  $N$ , which saturates to linear scaling behavior (and converge to the ML results) only for island exceeding  $N \sim 30$  molecules in this 2-dimensional model. Interestingly, the discrete spectrum of an island comprising a small number of molecule leads to a distinct structure in the current-voltage characteristics. While this is an obvious possibility, it is usually disregarded in theoretical analysis of experimental “single molecule” junctions.

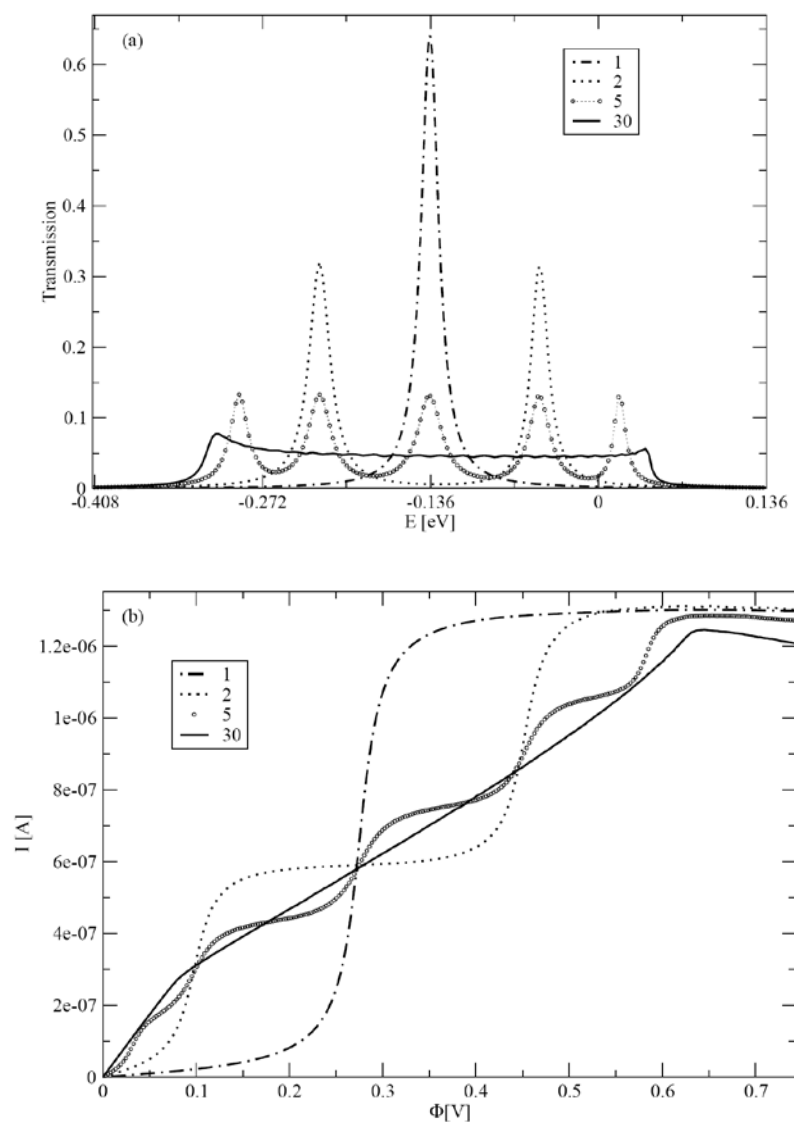


Fig. 10. The transmission coefficient (a) and the current-voltage characteristics (b) of 2-dimensional junctions comprising molecular islands of different sizes (expressed by the number of molecules  $N$ ). The

parameters used in these calculations are  $V^{(t)} = 1.1$  eV,  $V^{(m)} = 0.095$  eV,  $\varepsilon_m - \varepsilon_t = -0.136$  eV,  $V^{(mt1)} = 0.11$  eV (substrate),  $V^{(mt2)} = 0.055$  eV (probe) and  $S = 0.5$ .

## **7. Summary and conclusions**

The conduction properties of molecular junctions depend on structural and interaction parameters. In this review we have focused on effects associated with intermolecular interactions, as may be revealed in observations of the dependence of conduction on the number of conducting molecules; in the extreme case, comparing single molecules junctions to junctions based on molecular layers. In this review we have focused on several factors that affect this dependence: electrostatic screening, electrostatic interactions affecting molecule-substrate charge transfer, and intermolecular interactions affecting broadening of transmission resonances.

The individual or collective nature of molecular conduction often comes under discussion with respect to observation of apparent scaling of conduction with the number of molecules involved. We have pointed out, and demonstrated in model calculations, that such observations may depend on the nature of the molecular system. Simple linear scaling of the single molecule

behavior is expected only beyond some molecular cluster size that depends on the intermolecular interaction. In particular, in our simplified 2-dimensional calculation, and based on our (physically motivated) choice of short range interaction parameters, we have estimated this linear size to be of the order of  $\sim 30$  molecular sites. Again we emphasize that the conduction per molecule in these linear scaling regime may be quite different from that of the corresponding single molecule junction.

Finally, we point out that other collective molecular effects can influence molecular conduction and related transport properties. Of considerable interest are mechanical properties associated with the temperature dependence of molecular conduction (see figure 2) and heat conduction effects<sup>30</sup> that besides their intrinsic significance are importantly manifested in junction stability properties.

### **Acknowledgements**

We thank David Cahen and Ron Naaman for many helpful discussions. This research was supported by grants the Israel Science Foundation, the USA-Israel Binational Science Foundation, the Germany-Israel Foundation and the Schmidt Minerva Center for Supramolecular Chemistry. This paper is dedicated to Yosef Imry, an inspiring leader of our field.

**References**

- <sup>1</sup> H. B. Akkerman and B. de Boer, *J. Phys.: Cond. Mat.* 20 (1), 013001 (2008).
- <sup>2</sup> X. D. Cui, A. Primak, X. Zarate, J. Tomfohr, O. F. Sankey, A. L. Moore, T. A. Moore, D. Gust, G. Harris, and S. M. Lindsay, *Science* 294, 571 (2001).
- <sup>3</sup> B. Xu and N. J. Tao, *Science* 301 (5637), 1221 (2003).
- <sup>4</sup> J. G. Kushmerick, J. Naciri, J. C. Yang, and R. Shashidhar, *Nano Lett.* 3 (7), 897 (2003).
- <sup>5</sup> A. S. Blum, J. G. Kushmerick, S. K. Pollack, J. C. Yang, M. Moore, J. Naciri, R. Shashidhar, and B. R. Ratna, *The Journal of Physical Chemistry B* 108, 18124 (2004).
- <sup>6</sup> A. Salomon, D. Cahen, S. M. Lindsay, J. Tomfohr, V. B. Engelkes, and C. D. Frisbie, *Advanced Materials* 15, 1881 (2003).
- <sup>7</sup> Y. Selzer, L. Cai, M. A. Cabassi, Y. Yao, J. M. Tour, T. S. Mayer, and D. L. Allara, *Nano Letters* 5, 61 (2005).
- <sup>8</sup> R. Temirov, S. Soubatch, A. Luican, and F. S. Tautz, *Nature* 444 (7117), 350 (2006).
- <sup>9</sup> M. Magoga and C. Joachim, *Phys. Rev. B* 59 (24), 16011 (1999).
- <sup>10</sup> S. N. Yaliraki and M. A. Ratner, *J. Chem. Phys.* 109 (12), 5036 (1998).

- 11 N. D. Lang and P. Avouris, *Phys. Rev. B* 62, 7325 (2000).
- 12 Y.-H. Kim, J. Tahir-Kheli, P. A. Schultz, W. A. Goddard,  
and Iii, *Physical Review B (Condensed Matter and  
Materials Physics)* 73 (23), 235419 (2006).
- 13 A. Nitzan, M. Galperin, G.-L. Ingold, and H. Grabert, *J.  
Chem Phys.* 117 (23), 10837 (2002).
- 14 G. C. Liang, A. W. Ghosh, M. Paulsson, and S. Datta,  
*Phys. Rev. B* 69, 115302 (2004).
- 15 W. D. Tian, S. Datta, S. H. Hong, R. Reifengerger, J. I.  
Henderson, and C. P. Kubiak, *J. Chem. Phys.* 109 (7), 2874  
(1998).
- 16 M. Galperin, A. Nitzan, S. Sek, and M. Majda, *J.  
Electroanalytical Chem.* 550-551, 337 (2003).
- 17 D. Cahen, R. Naaman, and Z. Vager, *Advanced Functional  
Materials* 15 (10), 1571 (2005); G. Heimel, L. Romaner, E.  
Zojer, and J. L. Bredas, *Nano Lett.* 7, 932 (2007); D.  
Cornil, Y. Olivier, V. Geskin, and J. Cornil, *Adv. Function.  
Mat.* 17 (7), 1143 (2007); L. Romaner, G. Heimel, C.  
Ambrosch-Draxl, and E. Zojer, *Adv. Funct. Mater* 18, 3999  
(2008).
- 18 A. Natan, Y. Zidon, Y. Shapira, and L. Kronik, *Phys. Rev.  
B* 73 (19), 193310 (2006).
- 19 D. Deutsch, A. Natan, Y. Shapira, and L. Kronik, *J. Am.  
Chem. Soc.* 129 (10), 2989 (2007).

- 20 A. Natan, L. Kronik, H. Haick, and R T. Tung, *Advanced Materials* 19 (23), 4103 (2007).
- 21 S. Datta, W. D. Tian, S. H. Hong, R. Reifenberger, J. I. Henderson, and C. P. Kubiak, *Phys. Rev. Lett.* 79 (13), 2530 (1997).
- 22 N. D. Lang and P. Avouris, *Phys. Rev. Lett.* 84 (2), 358 (2000); P. S. Damle, A. W. Ghosh, and S. Datta, *Phys. Rev. B* 64, 201403 (2001); M. Brandbyge, J. L. Mozos, P. Ordejon, J. Taylor, and K. Stokbro, *Phys. Rev. B* 65 (16), 165401 (2002).
- 23 A. Bachtold, M. S. Fuhrer, S. Plyasunov, M. Forero, E. H. Anderson, A. Zettl, and P. L. McEuen, *Phys. Rev. Lett.* 84, 6082 (2000).
- 24 N. Mingo, J. Han, M. P. Anantram, and L. Yang, *Surface Science* 482 (485), 1130 (2001).
- 25 N. Gozlan and H. Haick, *J. Phys. Chem. C* 112, 12599 (2008); N. Gozlan, U. Tisch, and H. Haick, *J. Phys. Chem. C* 112, 12988 (2008); N. Peor, R. Sfez, and S. Yitzchaik, *J. Am. Chem. Soc.* 130, 4158 (2008).
- 26 A. Ulman., *An Introduction to Ultrathin Organic Films.* (Academic Press, San Diego, 1991).
- 27 A. Landau, A. Nitzan, and L. Kronik, *Journal of Physical Chemistry A* 113, 7451 (2009).

- 28 A. Landau, L. Kronik, and A. Nitzan, *Journal of Computational and Theoretical Nanoscience* 5, 535 (2008).
- 29 R. Landauer, *IBM J. Res. Dev.* 1, 223 (1957); S. Datta, *Electric transport in Mesoscopic Systems*. (Cambridge University Press, Cambridge, 1995).
- 30 Z. Liu and B. Li, *Phys. Rev. E* 76, 051118 (2007).